Procedia Manufacturing

Volume 1, 2015, Pages 804–813

43rd Proceedings of the North American Manufacturing Research Institution of SME http://www.sme.org/namrc

Prediction of Distortions in Hot Forged Martensitic Stainless Steel Turbine Blades by Numerical Simulation

Enrico Simonetto[1], Stefania Bruschi[1], Andrea Ghiotti[1*], Enrico Savio[1]

[1]*Department of Industrial Engineering, University of Padua, via Venezia 1,35131, Padova, Italy.*

enrico.simonetto.1@studenti.unipd.it, stefania.bruschi@unipd.it, andrea.ghiotti@unipd.it, enrico.savio@unipd.it.

Abstract

Hot forged parts characterized by thin sections may suffer geometric distortions during the cooling phase that force the process designers to work with significant machining allowances. The correct identification of the such defects during the process design might allow the proper set of the process parameters for their compensation and, therefore, the reduction of the allowances and the machining steps. The early computation of such distortions can be fulfilled by using thermal-mechanical-metallurgical models of both the forging and cooling phases, which must be calibrated through extensive experimental campaigns, involving both laboratory experiments and on-field measurements during industrial production.

The paper presents a coupled experimental and numerical approach to predict the geometrical distortions of turbine blades in martensitic stainless steel. The presented approach comprises both the development of the numerical models of the forging and cooling phases and their calibration using accurate material data. In order to validate the numerical models, the numerically predicted geometries are compared to those measured during cooling by using a newly developed laser scanning system devoted to high temperature measurements of complex-shaped parts just after the forging step and during all the cooling phases.

Keywords: Hot forging, Cooling, Turbine blades, Geometrical distortions, X20Cr13

Peer-review under responsibility of the NAMRI Scientific Committee

doi:10.1016/j.promfg.2015.09.067

1 Introduction

Hot forging of freeform components like turbine blades is often characterized by a quite limited repeatability in terms of the final geometry. Thus, additional heating steps, straightening operations, dimensional controls and machining operations are often needed and represent the main drawback of such process.

Turbine blades for applications in power plants can be successfully produced in different materials, but martensitic stainless steels actually represent one of the best solutions to manufacture components with excellent mechanical properties and moderate corrosion resistance (Fa-Cai, 2014). Unlike other stainless steels, the high carbon content allows phase transformations so that the mechanical properties of such steel can be changed by heat treatments (Nasery, 2011). In the last two decades the annual consumption of stainless steel has increased at a compound growth rate of 5%, surpassing the growth rate of other materials (Baddoo, 2008). Furthermore, due to their reduced thickness and complex freeform shape, hot forged turbine blades suffer geometric distortions during the cooling phase due to plastic deformations induced by thermal gradients, and to transformation plasticity effects as a consequence of the phase changes. Such phenomena lead to an overall increase of costs due to subsequent machining operations necessary to obtain the final geometry and to additional heat treatments to assure the desired microstructure. Ideally, the estimation of the distortions should be made from the earliest stages of the design process, in order to choose the appropriate process parameters to minimize the number of subsequent operations.

The problem of the process optimization can be addressed through numerical simulation of the entire process chain, with models that include coupled thermo-mechanical–metallurgical effects. Different models are proposed in scientific literature, which take into account the effects of these coupled contributions, some applied to cylindrical specimens hardened in a furnace and verified by 2D simulations (Liu, 2003) (Lee, 2007), other verified by measurements through vision systems during the cooling (Claudinona, 2002). There are also models applied to non-axisymmetric components (Da Silva, 2012) and also with coupled deformation and cooling phases (Lu Xian, 2001), always applied through two-dimensional numerical simulations. Other authors refers to thermo-mechanical-metallurgical approaches specifically developed for the calculation of the distortions in the forming and cooling of turbine blades, applied through three-dimensional models (Bruschi, 2008), (Bariani, 2004), but no direct validation of the simulated geometries through measurements at elevated tempratures carried out just at the end of the deformation or duling the cooling phase have been provided yet. Such approaches require the integration of different experimental techniques in order to obtain a reliable calibration of the numerical models, with attention to: (i) the mechanical behaviour, through the determination of the material flow stress at the mechanical and temperature conditions of the processes, (ii) the microstructural behaviour, through the knowledge of the phase transformations due to the thermal changes the material is subjected to, and (iii) the thermal behaviour, that is governed by the boundary conditions between the die and the component during the deformation and post-deformation phases. In addition to their complexity, a review of the scientific literature shows that the proposed models are often verified only with the geometric parameters measured at the end of the cooling phase, due to the difficulties in performing direct measurements at elevated temperatures.

The paper presents an integrated approach for the prediction of the distortions that may affect hot forged turbine blades and its validation through in-line measurement of the blade geometry at elevated temperatures. Thanks to a newly developed laser scanner prototype (Schöch, 2014), capable of measuring the geometry of complex-shape parts at temperatures up to 1200 °C in less than 10 s, different cross sections of the hot forged blade aerofoil were measured during the cooling phase just after the deformation. The experimental results were finally compared to the numerical ones, obtained by a fully coupled thermal-mechanical-metallurgical FE model, which was developed and properly calibrated through laboratory experiments.

2 Application case

The application case refers to the hot forging of stainless steel turbine blades for energy plants carried out on a double-effect hammer. The used material is the martensitic stainless steel X20Cr13, which is commonly used in applications that require high strength at elevated temperatures together with a good corrosion resistance. The chemical composition and the mechanical properties of the material in the as-delivered conditions are reported in Table 1. The initial size of the austenitic grain, obtained through micrographic analysis after application of the McQuaid-Ehn procedure, which requires a solid carbo-cementation (for eight hours at 927 °C), able to point out the edges of the austenitic grain, is equal to 18 μm (ASTM 9).

Table 1: Chemical composition of X20Cr13 and mechanical properties at room temperature.

Element	C	Si	Mn	Cr
Wt%	0.20	0.40	0.40	12.50
Characteristic	$R_{p0.2}$ [MPa]	R_m [MPa]	A_5 [%]	KV [J]
	≥ 500	750 ÷ 1050	≥ 12	≥ 15
Martensitic stainless steel with a relative high carbon content to allow heat treatment. Resistant to corrosive action of water and steam, after surface treatment of grinding or polishing.				

The turbine blade measures 900 mm x 220 mm x 150 mm, for a total weight of 65 kg. The process chain consists of three main stages: after the initial preforming stage, which basically consists of a swaging operation carried out on an hydraulic press, the billet is heated up to 1100 °C in a gas furnace and forged in about 20 blows on a 400 kJ double-effect hammer, equipped with a pneumatic system to increase the total deformation energy and heated dies. The blades are forged using the lubricant Acheson Deltaforge31. Finally, the formed blade is positioned on a transfer bench and cooled down to room temperature for a sufficient time to ensure that the correct phase transformations occur. The flowchart of the process is reported in Fig. 1.

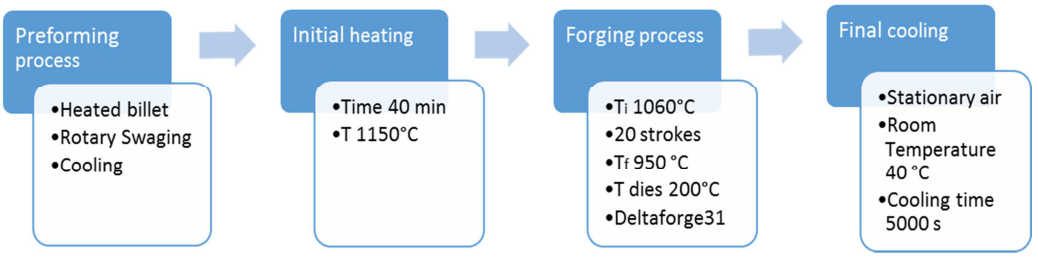

Fig. 1: Flow chart of the process chain with the main process parameters.

3 Material

3.1 Flow stress

The material flow stress was investigated in the same range of temperatures and strain rates of the industrial process. Hot compression tests, performed on the thermo-mechanical simulator Gleeble 3500^{TM}, were carried out on cylindrical specimens of X20Cr13. Each specimen was subjected to the same thermal cycle experienced in the gas furnace by the blades so as to obtain the same austenitic grain on the test samples and on the blank under examination. Table 2 shows the experimental plan

for the material characterization that was derived by the industrial-measured process parameters. Fig. 2 shows the results of the experiments, with reference to the strain rate and temperature influence: at a fixed temperature, an increase of the strain rate from $1s^{-1}$ to $50s^{-1}$ determine an increase of the flow stress up to 60% (see Fig. 2a) while decreasing the test temperature down to 800°C, that was fixed as the lower limit for the process before reheating, increase the flow stress up to 50% compared to the initial forging temperature. Through a non-linear regression analysis of the experimental data, the constants of the Hansel-Spittel equation (1), which was chosen to be implemented in the FE code for the simulations, were calculated (see the results reported in Table 2). To take into account the softening material behaviour at higher strains, the 9 coefficients model was implemented in the simulations according to the formula,:

$$\sigma = A \cdot e^{m_1 T} \cdot T^{m_9} e^{m_4/\varepsilon} \cdot (1+\varepsilon)^{m_5 T} \cdot e^{m_7 \varepsilon} \cdot \dot{\varepsilon}^{m_3} \cdot \dot{\varepsilon}^{m_8 T} \quad (1)$$

where σ is the Von Mises stress in [MPa], ε the strain, $\dot{\varepsilon}$ the strain rate in [s-1]. The Hensel-Spittel equation was chosen since it allows the best fitting of the curves and the faster convergence of the numerical simulations.

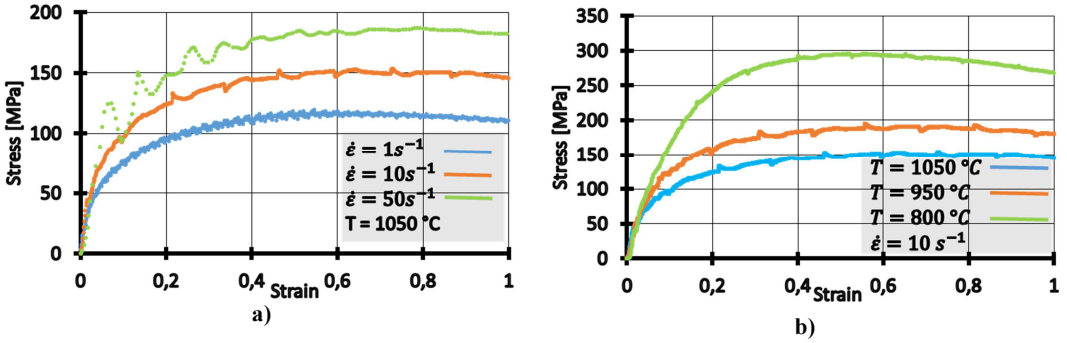

Fig. 2: X20Cr13 sensitivity to strain rate at T = 1050 °C (a), sensitivity to temperature at strain rate = 10 s^{-1} (b).

Table 2: Test conditions and Hansel-Spittel model constants.

Material	Temperature [°C]	ε max	$\dot{\varepsilon}$ [s^{-1}]	
X20Cr13	1050	1	1	
	950		10	
	800		50	
Hansel Spittel Constants				
A [MPa]	m_1	m_2	m_3	m_4
1.69E+08	-0.00099	0.43924	-0.11564	-0.01146
m_5	m_6	m_7	m_8	m_9
-0.00026	0.00000	-0.62434	0.000224	-1.78362

3.2 Phase transformation

The distortions incurred during the cooling, resulting in significant changes in the blade final sections geometries, are influenced (i) by the phase transformations phenomena (each phase differs for the microstructure and the specific volume), (ii) by the thermal expansion coefficient and (iii) by the transformation plasticity that is a plastic deformation due to the coupled effect of phase change in presence of residual stresses, also inferior to the material yield stress. A review of the scientific literature shows that different models have been proposed for the characterization of phase

transformations of austenitic steels during cooling (Taleb, 2001) (Taleb, 2003). In recent years, several models have been applied to austenitic and martensitic stainless steel, but they do not take into account the same process parameters of the industrial case examined (Samantaray, 2011) (Mark, 2014).

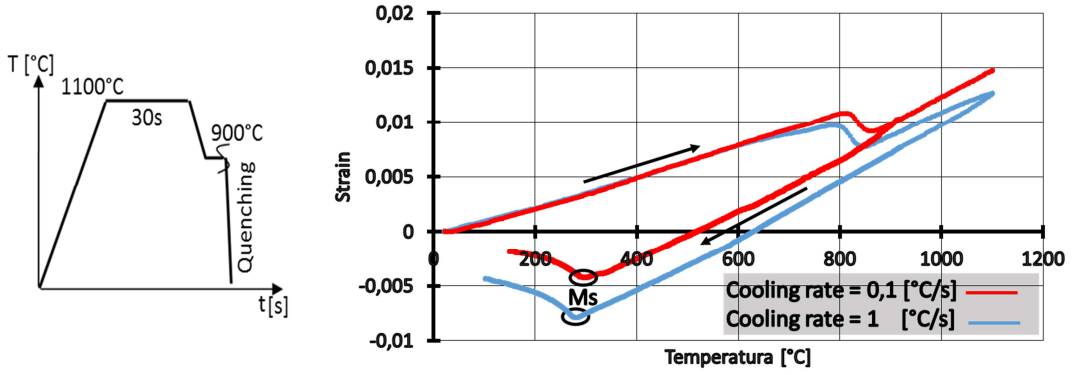

(a) (b)

Fig. 3: Thermal cycle applied to X20Cr13 specimens (a), and dilatometric curves (b).

A tensile test set-up on the Gleeble 3500^{TM}, equipped with a dilatometer to monitor the phase transformation onset, was used for the investigation of the phenomena related to the phase transformation: thermo-mechanical experiments were focused on the austenite to martensite transformation, responsible for the cooling deformations. The microstructure analysis of the turbine blade shows a grain size between 18 μm and 13 μm (ASTM 9 – 10); the same size was obtained on the specimens when subjected to the thermal cycle show in Fig. 3a. The specimens were quenched at different cooling rates, chosen according to the ones adopted in the industrial process, between 0.1 and 1 °C/s. The only phase transformation taking place in such range is the martensitic one, responsible for the increase of volume of the sample at about 280 °C, during the cooling phase, as show in Fig. 3b. The coefficients of linear expansion α for the different phases were determined by calculating the slope of the straight lines in the curves shown in Fig. 3b.

The same thermal cycles were used to determine the portion of the CCT curves relevant to the industrial cooling rates, from which the TTT curves, used in the numerical model, were determined according to the procedure described in (Rios, 2005). The determination of the transformation

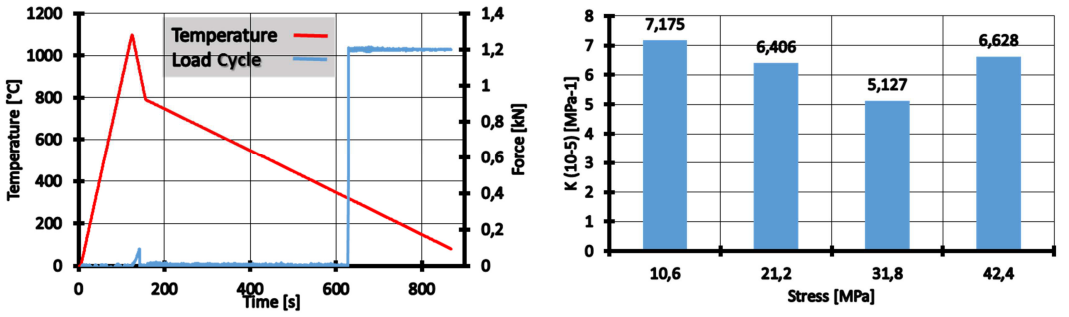

(a) (b)

Fig. 4: (a) Temperature and load cycles applied to the specimens, and (b)martensite transformation plasiticity coefficents as a function of the applied stress.

plasticity coefficients requires both thermal and mechanical tests; firstly, a purely thermal cycle is applied to the specimen in order to determine the thermal component of the total strain ε^{th}; secondly, a load cycle, as show in Fig. 4a, is superimposed to the thermal one, just before the onset of the martensitic transformation, to evaluate the total strain ε^{tot}. The transformation plasticity strain is derived from the following:

$$\varepsilon^{tp} = \varepsilon^{tot} - \varepsilon^{th} - \varepsilon^{el} \tag{2}$$

where the elastic strain $\varepsilon^{el}$is calculated from the Hooke's law.

The transformation plasticity strain is correlated to the applied stress through the transformation plasticity coefficient *k* and the volume proportion of transformed phase Z:

$$\varepsilon^{tp} = kg(Z)\sigma \tag{3}$$

The values of ε^{tp} are reported in Fig. 4b as function of the applied stress level.

4 FE model

In order to analyse the final distortions occurring to the aerofoil blade, the finite element software Forge 2011[TM] was used. Both the forging and the cooling phases were simulated using a coupled thermo-mechanical-metallurgical model of the forming process, as described in the following paragraphs.

4.1 Deformation phase

The deformation process was simulated using a three-dimensional model with non-deformable dies. The initial temperature of the workpiece is set equal to 1060°C, as it was measured in the forging plant, while the dies temperature was set at 200°C in agreement with the industrial process. The material model was obtained according to the procedure explained in paragraph 3, using the Hansel-Spittel equation with 8 coefficients. As the deformation is conducted with lubrication, a Tresca factor equal to 0.4 was considered. At the end of the forging process, before being removed, the blade is left

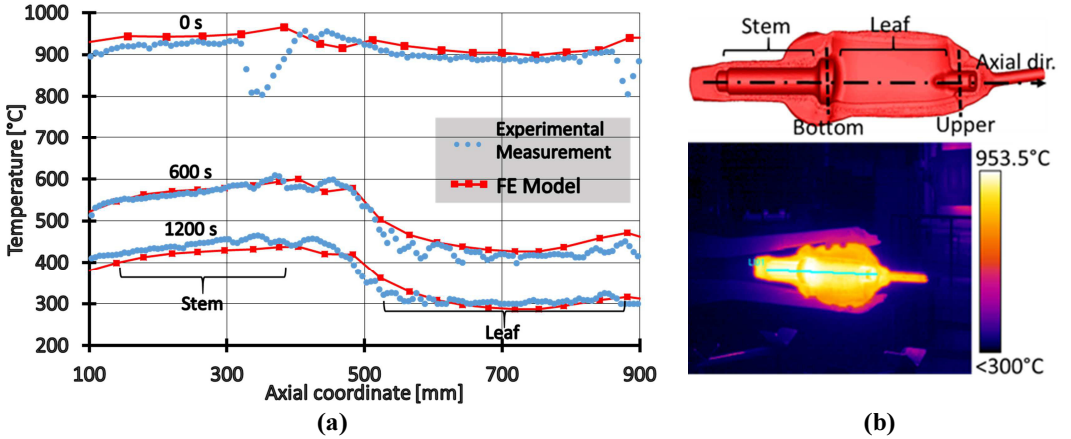

Fig. 5: Surface temperatures along the axial direction at the end of the forging phase (0 s) and during the cooling phase (600, 1200 s) (a), temperature maps acquired through infrared thermo-camera (b).

in contact with the lower die for 20 s to take into account the dwell time before removing the blade: this cooling phase on the dies was simulated and chained to the previous one. An accurate evaluation of the Heat Transfer Coefficient (HTC) is fundamental to predict the correct thermal field in the blades during the forging and cooling phases until room temperature.

To obtain reliable value of the HTCs, surface temperature measurements were carried out in the industrial plant by utilizing an infrared thermo-camera, as shown in Fig. 5b. The best-suited HTC coefficients between the billet and the tools during the deformation process were calculated through the application of an already developed inverse analysis procedure (Bariani, 2002). A value of HTC equal to 500 W/m^{2}K with dies and equal to 10 W/m^{2}K with the environment permitted to have the best matching between numerically calculated and measured surface temperatures at the end of the deforming phase, as shown in Fig. 5a. The calculated temperature profiles fit well on the aerofoil zone, while some inaccuracies on the bottom and upper sections were considered negligible for the purpose of the investigations. They might probably depend on the presence of oxides on the blade surface that affected the experimental measurements.

4.2 Cooling phase

Just after the forging phase, the blades are cooled down to room temperatures on racks in stationary air conditions. Being limited the area of the blades in contact with the rack, the thermal exchange between the blades and the rack was not considered. A value of HTC equal to 10 W/m²K was set with the environment, calculated by inverse analysis minimizing the offset with the experimental measurements carried out at the factory plant. Fig. 5 shows an example of the experimental measurements just after the forming phase and the comparison between the temperatures calculated with the FE model and the ones experimentally measured. The temperatures were collected along the axial direction of the surface at different times of the cooling phase, respectively at the beginning of the cooling, after 600 s and after 1200 s. The maximum error with the experimental data was 5%, concentrated in the area of the stem.

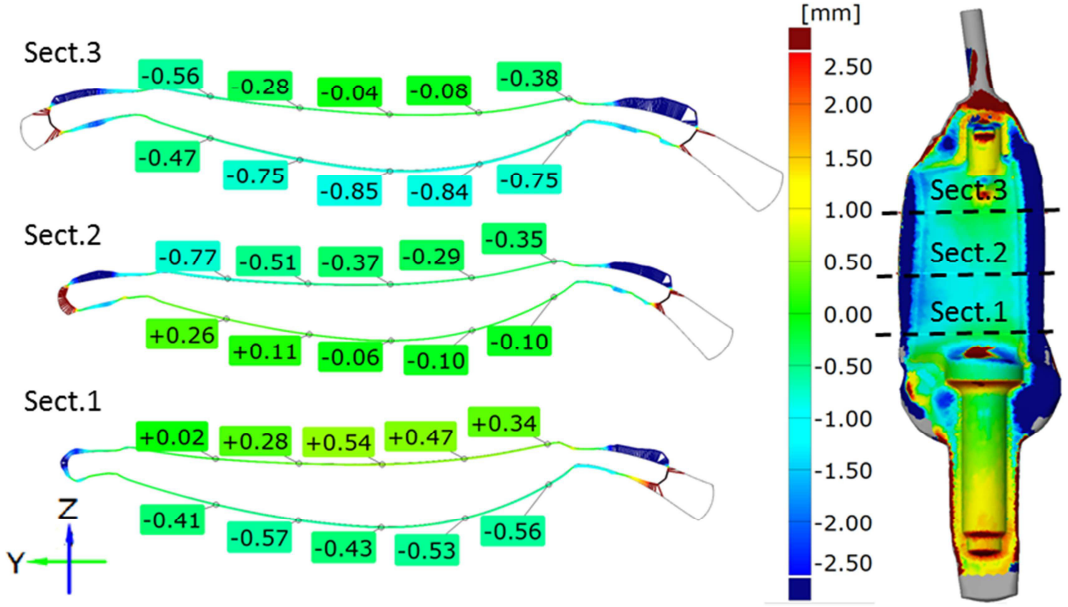

Fig. 6: Cross sections of analysis and comparison between the cross sections calculated by the FE model and the experimental results at the end of the forging process.

5 Results and discussion

The comparison between the numerical and experimental results was focused on the aerofoil sections, where the effect of thermal dilatation and microstructural changes are more evident. Thanks to a newly developed 3D laser scanner prototype, the hot forged aerofoil blade was measured during the cooling phase down to room temperature. The alignment between the measured surfaces and the calculated surfaces were realized by the GOM Inspect ^{TM} software, using a least square analysis that is adversely affected by the differences in the flash development. Fig.6 shows the blade cross sections taken as reference for the evaluation of the geometries obtained by numerical simulation and the experimental measurements and the map of the gaps between the two geometries at the end of the forging process. The comparison shows a good agreement with the FE results. The largest error of 0.85 mm was detected for the case of the cross section 3, probably due to the bigger difference in the flash development. For the cross sections 1 and 2, which have lower difference in the flash development, the FE results has a better matching with the experimental data. Several factors can be considered to explain the differences between the numerical and experimental results, such as the dies wear, the elastic deflection of the dies and the press, the positioning of the billet on the dies that is made by the operator. The largest discrepancy of the numerical results was detected in the evaluation

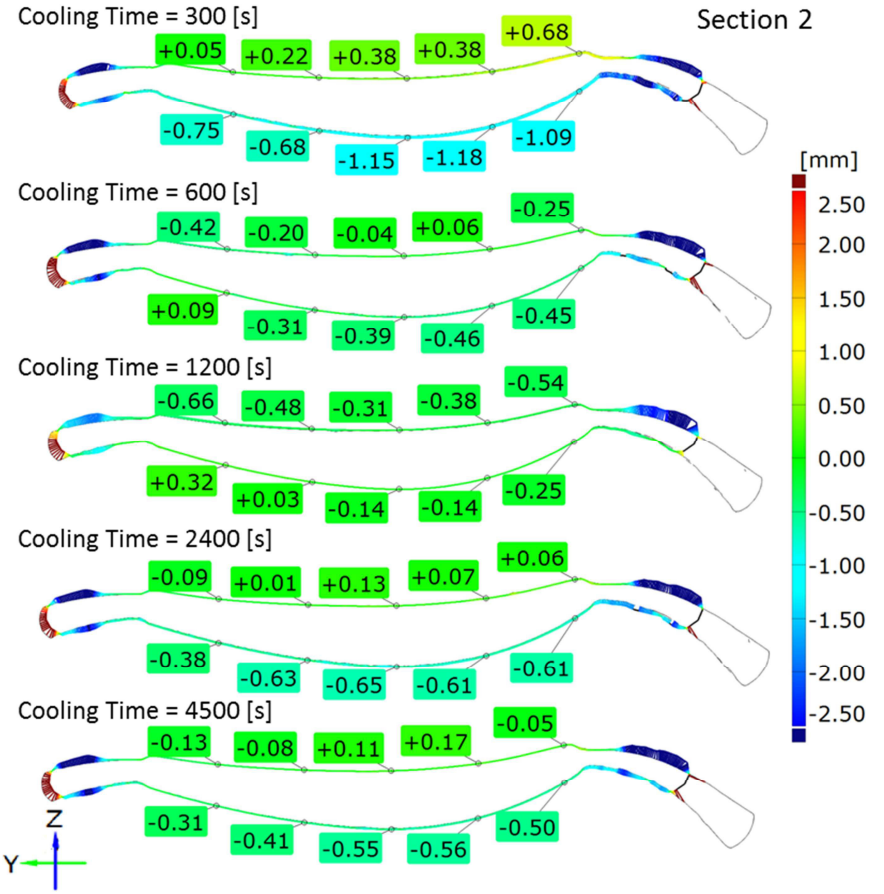

Fig. 7: Comparison between the cross sections 2 calculated by the FE model and the experimental measurements at different cooling times.

of the flash, which was overestimated in the FE analyses.

Fig. 7 shows the comparison between the FE calculated and the measured cross-section geometries at different times of the cooling, respectively at 300 s, 600 s, 1200 s, 2400 s and 4500 s. The experimental measurements were obtained by the 3D measurements of the blade during the cooling. The results of the simulations are in good agreement with the experimental measurements, with a maximum difference of 1.18 mm after 300 s of cooling time. This difference, slightly higher than the other steps, can be attributed to a delay of the phase transformations simulation in the numerical case compared to the real phenomenon. The final result of the simulations after 4500 s, when all the phase transformations occurred, is very close to the experimental measurement showing the good predictive capabilities of the numerical model calibrated through the proposed methodology.

6 Conclusions

The paper presents an approach for the prediction of the final geometry of a complex component forged at elevated temperature and cooled down in stationary air. A newly developed 3D laser scanner prototype was used to measure the geometry of hot forged turbine blades during the cooling phase down to room temperature after deformation. The experimental results were finally compared to the numerical ones, obtained by a fully coupled thermal-mechanical-metallurgical FE model, which was developed and properly calibrated through laboratory experiments.

A 3D numerical model of the forging and the cooling phases was set up and properly calibrated through on-field measurements and laboratory experiments. The results of the simulations proved to be in excellent agreement with the measurements of the actual blade, also along the aerofoil that is the area subjected to the greater distortions. The largest errors in the range of 1.18 mm were detected in the upper part of the aerofoil due to the difference between the flash developments. So, the approach has shown a good capability of reproducing the industrial process and high potentiality for the possibility to optimize the dies design and process parameters.

References

Baddoo NR. Stainless steel in construction: A review of research, applications, challenges and opportunities. *Journal of Constructional Steel Research* 2008; 44(8): 1199-1206.

Bariani PF, Berti G, Dal Negro T and Masiero S. Experimental evaluation and FE simulation of thermal cycle at tool surface during cooling and deformation phases in hot and warm forging operations. *Annals of CIRP* 2002; 51(1): 219-222.

Bariani PF, Bruschi S and Dal Negro T. Integrating physical and numerical simulation techniques to design the hot forging process of stainless steel turbine blades. *International Journal of Machine Tools and Manufacture* 2004; 44: 945-951.

Bruschi S and Ghiotti A. Distortions induced in turbine blades by hot forging and cooling. *International Journal of Machine Tools & Manufacture* 2008; 48: 761-767.

Claudinona S, Lamesle P, Orteu JJ and Fortunier R. Continuous in situ measurement of quenching distortions using computer vision. *Journal of Materials Processing Technology* 2002; 122: 69-81.

Da Silva AD, Pedrosa TA, Gonzalez-Mendez JL, Jiang X, Cetlin PR and Altan T. Distortion in quenching an AISI 4140 C-ring – Predictions and experiments. *Materials & Design* 2012; 42: 55-61.

Dipti Samantaray, Sumantra Mandal, Bhaduri AK, Venugopal S and Sivaprasad PV. Analysis and mathematical modelling of elevated temperature flow behaviour of austenitic stainless steels. *Materials Science and Engineering* 2011; 528: 1937-1943.

Fa-Cai Ren, Jun Chen and Fei Chen. Constitutive modeling of hot deformation behavior of X20Cr13 martensitic stainless steel with strain effect. *Transactions of Nonferrous Metals Society of China* 2014; 24 (5): 1407-1413.

Lee KO, Kim JM, Chin MH and Kang SS. A study on the mechanical properties for developing a computer simulation model for heat treatment process. *Journal of Materials Processing Technology* 2007; 128 (1-3): 65-72.

Liu CC, Xu XJ and Liu Z. A FEM modeling of quenching and tempering and its application in industrial engineering. *Finite Elements Analysis and Design* 2003; 29(11): 1053-1070.

Lu Xian and Balendra R. Temperature-related errors on aerofoil section of turbine blade. *Journal of Materials Processing Technology* 2001; 115(2): 240.

Mark AF, Moat R, Forsey A, Abdolvand H and Withers PJ. A new method for quantifying anisotropic martensitic transformation strains accumulated during constrained cooling. *Materials Science&Engineering* 2014; 611: 354-361.

Nasery Isfahany A, Saghafian H and Borhani G. The effect of heat treatment on mechanical properties and corrosion behavior of AISI420 martensitic stainless steel. *Journal of Alloys and Compounds* 2014; 509 (9): 3931-3936.

Rios PR. Relationship between non-isothermal transformation curves and isothermal and non-isothermal kinetics. *Acta Materialia* 2015; 53: 4893-4901.

Schöch A, Salvadori A, Germann I, Balemi S, Bach C, Ghiotti A, Carmignato S, Maurizio A and Savio E. Fast measurement of freeform parts at elevated temperature using laser-triangulation principle. *11th IMEKO TC14 Symposium on Laser Metrology for Precision Measurement and Inspection in Industry* 2014.

Taleb L, Cavallo N and Waeckel F. Experimental analysis of transformation plasticity. *International Journal of Plasticity* 2001; 17: 1-20.

Taleb L and Sidoroff F. A micromechanical modeling of the Greenwood–Johnson mechanism in transformation induced plasticity. *International Journal of Plasticity* 2003; 19: 1821-1842.